Helical Electron-Beam Microbunching by Harmonic Coupling in a Helical Undulator

E. Hemsing,[1] P. Musumeci,[1] S. Reiche,[1] R. Tikhoplav,[1] A. Marinelli,[1,2] J. B. Rosenzweig,[1] and A. Gover[3]

[1]*Particle Beam Physics Laboratory, Department of Physics and Astronomy University of California Los Angeles, Los Angeles, California 90095, USA*

[2]*Università degli Studi di Roma "La Sapienza", Via Antonio Scarpa 14, Rome, 00161, Italy*

[3]*Faculty of Engineering, Department of Physical Electronics, Tel-Aviv University, Ramat-Aviv 69978, Tel-Aviv, Israel*

(Received 13 August 2008; published 29 April 2009)

Microbunching of a relativistic electron beam into a helix is examined analytically and in simulation. Helical microbunching is shown to occur naturally when an *e* beam interacts resonantly at the harmonics of the combined field of a helical magnetic undulator and an axisymmetric input laser beam. This type of interaction is proposed as a method to generate a strongly prebunched *e* beam for coherent emission of light with orbital angular momentum at virtually any wavelength. The results from the linear microbunching theory show excellent agreement with three-dimensional numerical simulations.

DOI: 10.1103/PhysRevLett.102.174801 PACS numbers: 41.60.Cr, 42.50.Tx, 42.60.Jf, 42.65.Ky

A relativistic electron beam (*e* beam) that is subject to the free-electron laser (FEL) instability becomes microbunched in density and velocity at the resonant interaction wavelength, and at harmonics. The modulated *e* beam can then be used to emit radiation in various kinds of radiation schemes that preserve the characteristic frequency and geometry of the microbunching in the *e* beam. In general, the microbunching interaction generates a purely longitudinal modulation, such that the subsequent radiative process produces emission at, or near, the fundamental transverse optical mode. The range of modulation wavelengths obtainable in modern devices make this technique appealing for the generation of light with wavelengths that span many orders of magnitude. However, in some cases one may wish to produce radiation with the modulated beam that has a specific higher-order phase or intensity structure. Depending on the emission process, the *e* beam must be prepared with the correct microbunching structure in the modulator. Here we examine a simple modulator arrangement that generates a helically microbunched *e* beam, such that the electrons are arranged in a helix (or multiply twisted helices) about the longitudinal axis. Such a beam can be used for generation of coherent light that carries orbital angular momentum (OAM) as a result of the imprinted helical *e* beam density distribution on the optical phase.

Light that carries OAM is a subject of intense research for a myriad of applications [1–5]. Coherent OAM modes allow the possibility of light-driven micromechanical devices or the use of torque from photons as an exploratory tool [6]. Laguerre-Gaussian (LG) modes of free-space propagation are of particular interest since they are known to possess a well-defined value of angular momentum $l\hbar$ per photon due to an azimuthal component of the linear momentum [7]. Emission of OAM light with an *e* beam may be accomplished through a variety of radiation processes, including harmonic emission from an FEL [8] or through coherent transition radiation [9] or superradiant FEL emission [10,11] with helically microbunched beams. Modes of this type may be particularly relevant for study with modern optical and next-generation x-ray FELs with the ability to probe the structure of matter down to Å length and attosecond time scales. For future FEL light sources, the ability to directly generate intense higher-order LG modes *in situ* would further extend the experimental and operational capabilities.

In this Letter, we propose a scenario for generating a helically microbunched *e* beam which utilizes harmonic coupling in a helical undulator. We show that microbunching of this type may be easily performed with an axisymmetric EM seed input in the modulator section of an optical klystron [12]. The helical beam can then be used as a source of OAM radiation in a downstream radiator. A linear analysis of the harmonic bunching process is developed in which the input field and density modulation are treated as superpositions of orthogonal modes [13,14], and the beam couples at harmonics via field gradients in the input laser beam. Simple symmetry arguments are employed to clearly delineate the spatial dependence of the harmonic fields that couple to the *e* beam. The method also illustrates the geometric structure of the resonant phase for arbitrary harmonics, the mode coupling for a cylindrically symmetric *e* beam, and the resulting density and velocity modulations excited in the *e* beam during the interaction. Selection rules are also derived for coupling between azimuthal modes in the *e* beam (l) and in the field (l') at harmonics (h). These rules apply both to the modulator setup described here and to harmonic radiation in a FEL with a cold beam.

The interaction between the *e* beam and the input radiation field in an undulator operating as a buncher can be described analytically using standard linearized FEL equations in the small-signal regime if the radiation fields are injected with sufficient power (or the interaction length is

short enough) that the total field energy is unaffected by the e beam throughout interaction. The fields are assumed to be dominantly transverse. The electric field is given by the modal expansion

$$\mathbf{E}_\perp(\mathbf{r},t) = \mathrm{Re}\left[\sum_q C_q(z)\tilde{\mathcal{E}}_{\perp q}(\mathbf{r}_\perp)\hat{\mathbf{e}}_\perp e^{i[k_{zq}(\omega)z-\omega t]}\right], \quad (1)$$

where $\tilde{\mathcal{E}}_{\perp q}$ is an eigenfunction of an infinite, ideal wave guide (or optical fiber), $C_q(z)$ is the mode amplitude, $\hat{\mathbf{e}}_\perp$ is the field polarization vector and $k_{zq}(\omega)$ is the axial wave number of the mode q at the frequency ω. The TEM modes are orthogonal and normalized, with mode power $P_q\delta_{q,q'} = (k_{zq}(\omega)/2\mu_0\omega)\,\mathrm{Re}[\int \tilde{\mathcal{E}}_{\perp q}\tilde{\mathcal{E}}^*_{\perp q'}d^2\mathbf{r}_\perp]$, where $\mu_0 = 1/c^2\epsilon_0$ is the permeability of free-space. The total power in the input field is then $P_T = \sum_q |C_q(0)|^2 P_q$.

The e beam is described in a linear fluid model with density distribution

$$n(\mathbf{r},t) = n_0 f(\mathbf{r}_\perp) + \mathrm{Re}[n_1(\mathbf{r})e^{i\omega(z/v_0-t)}], \quad (2)$$

where n_0 is the electron density, $v_0 = \beta_z c$ is the longitudinal e beam velocity, $f(\mathbf{r}_\perp)$ is the transverse density profile of the e beam and $n_1(\mathbf{r})$ is the spatial density perturbation. The transverse variation of the charge density is assumed small compared with the longitudinal variation. With the Lorentz force equation for a single component plasma fluid in the presence of both the magnetostatic undulator field $\mathbf{B}_w = \mathrm{Re}\{|\tilde{\mathcal{B}}_w|\hat{\mathbf{e}}_w e^{-ik_w z}\}$ and the electromagnetic input fields [Eq. (1)], the density evolution equation in the cold-beam limit is written as [10]

$$\left[\frac{\partial^2}{\partial z^2} + \theta_p^2 f(\mathbf{r}_\perp)\right] n_1(\mathbf{r}) = -\hat{g}_\perp \theta_p^2 f(\mathbf{r}_\perp)\frac{\epsilon_0 cK}{2\gamma e\omega}\sum_{q'} C_{q'}(z) \times [k_{zq'} + k_w]^2 \tilde{\mathcal{E}}_{\perp q'}(\mathbf{r}_\perp)e^{-i\theta^{(1)}_{q'}z}, \quad (3)$$

where $\theta_p = \sqrt{e^2 n_0/\gamma\gamma_z^2\epsilon_0 m_e v_0^2}$ is the relativistic longitudinal plasma wave number and $\theta^{(h)}_{q'} = \omega/v_0 - (k_{zq'}(\omega) + hk_w)$ is the detuning of the input mode relative to the e beam energy at the harmonic h. The harmonic frequencies at resonance are $\omega^{(h)} = 2hk_w c\gamma_z^2$, with $\gamma_z^2 = (1-\beta_z^2)^{-1}$, $\gamma^2 = \gamma_z^2(1+K^2)$, $K = e|\tilde{\mathcal{B}}_w|/m_e c k_w$ is the undulator parameter, $|\tilde{\mathcal{B}}_w|$ is the field amplitude of the undulator and $\lambda_w = 2\pi/k_w$ is the undulator wavelength. We neglect the nonlinear contribution of the input field in the small-signal approximation $(K_f/K)^2 \ll 1$ where $K_f = e|\mathbf{E}_\perp|/\omega m_e c$. Polarization alignment between input EM field and the electron motion in the undulator is given by $\hat{g}_\perp = \hat{\mathbf{e}}_\perp \cdot (\hat{\mathbf{e}}_z \times \hat{\mathbf{e}}^*_w)$, where the polarization vector of the helical undulator is

$$\hat{\mathbf{e}}_w = (\hat{\mathbf{e}}_x \pm i\hat{\mathbf{e}}_y)/\sqrt{2}, \quad (4)$$

which corresponds to either right (+) or left (−) circular polarization along z. Maximal coupling from polarization alignment ($\hat{g}_\perp = 1$) is obtained when the optical field polarization is $\hat{\mathbf{e}}_\perp = \hat{\mathbf{e}}_z \times \hat{\mathbf{e}}_w$ which describes a *left*-circularly polarized wave (positive helicity [15]) matched with a *right*-circularly polarized undulator.

The e beam is coupled to the input field modes through the ponderomotive fields, given by the right-hand side of Eq. (3). Since the resonant interaction is sustained near the synchronous condition only for the first harmonic ($\theta^{(1)}_{q'} \simeq 0$), there is no higher-harmonic coupling of the electron beam to first order. Coupling at higher harmonics can be excited in a cold beam through the higher-order resonant interaction between the electrons and the gradients of the EM fields. This contribution is calculated by Taylor expanding the field modes $\tilde{\mathcal{E}}_{\perp q}$ about the average centroid trajectory of an electron $\bar{\mathbf{r}}_\perp$,

$$\tilde{\mathcal{E}}_{\perp q}(\mathbf{r}_\perp) = \sum_{n=0}^{\infty}\frac{1}{n!}[\mathrm{Re}(\tilde{\mathbf{r}}_{\perp w}e^{-ik_w z})\cdot\bar{\nabla}]^n\tilde{\mathcal{E}}_{\perp q}(\bar{\mathbf{r}}_\perp), \quad (5)$$

where the transverse coordinate of an electron is $\mathbf{r}_\perp = \bar{\mathbf{r}}_\perp + \mathrm{Re}[\tilde{\mathbf{r}}_{\perp w}e^{-ik_w z}]$ and $\bar{\nabla}$ is the gradient operator which acts on $\bar{\mathbf{r}}_\perp$. The electron wiggling amplitude is $\tilde{\mathbf{r}}_{\perp w} = (K/k_w\gamma\beta_z)\hat{\mathbf{e}}_z \times \hat{\mathbf{e}}_w$. Insertion of Eq. (5) into Eq. (3) introduces additional oscillatory wiggling terms which couple to higher-harmonic resonances. In the regime where $|\tilde{\mathbf{r}}_{\perp w}|$ is much smaller than the characteristic transverse e beam size r_0, we approximate $\bar{\mathbf{r}}_\perp \simeq \mathbf{r}_\perp$ in Eq. (5) and obtain an expression for the Taylor expanded harmonic field components that are resonant with the integer harmonics h,

$$\tilde{\mathcal{E}}^{(h)}_{\perp q}(\mathbf{r}_\perp) = e^{\mp i(h-1)\phi}\left[\partial_r \mp \frac{i}{r}\partial_\phi\right]^{h-1}\sum_{m=0}^{\infty}\frac{(-1)^m}{m!(m+h-1)!} \times \left(\frac{\pm iK}{2\sqrt{2}k_w\gamma\beta_z}\right)^{2m+h-1}\nabla_\perp^{2m}\tilde{\mathcal{E}}_{\perp q}(\mathbf{r}_\perp), \quad (6)$$

where $\nabla_\perp^2 = \frac{1}{r}\partial_r(r\partial_r) + \frac{1}{r^2}\partial_\phi^2$ is the transverse Laplacian operator. The higher-order terms ($m > 0$) in the Taylor series can be neglected if the wiggle amplitude of the electrons is small compared to the optical beam size. With Eq. (6), harmonic interactions are described in Eq. (3) by replacing $\tilde{\mathcal{E}}_{\perp q'}(\mathbf{r}_\perp)e^{-i\theta^{(1)}_{q'}z}$ with $\tilde{\mathcal{E}}^{(h)}_{\perp q'}(\mathbf{r}_\perp)e^{-i\theta^{(h)}_{q'}z}$.

It is convenient to express the density perturbation $n_1(\mathbf{r})$ as a sum over the expansion eigenmodes such that the orthogonality of the basis can be used to compactly write the density evolution Eq. (3) in terms of spatial modulation amplitudes. The density modulation expansion is,

$$n_1(\mathbf{r}) = \frac{k_w\epsilon_0}{e}\sum_j a_j(z)\tilde{\mathcal{E}}_{\perp j}(\mathbf{r}_\perp). \quad (7)$$

The substituted harmonic terms in Eq. (3) are then multiplied by $\tilde{\mathcal{E}}^*_{\perp q}(\mathbf{r}_\perp)$ and integrated over the transverse coordinates, yielding an expression for the evolution of the density mode amplitudes at harmonics:

$$\frac{d^2}{dz^2}a_q(z) + \theta_p^2 \sum_j \mathbb{F}_{q,j} a_j(z) = -\sum_{q'} \mathbb{D}^{(h)}_{q,q'} C_{q'}(z) e^{-i\theta^{(h)}_{q'} z}. \tag{8}$$

The coupling of the e beam with arbitrary transverse density distribution $f(\mathbf{r}_\perp)$ to the harmonic fields is given by the coupling coefficient

$$\mathbb{D}^{(h)}_{q,q'} = \hat{g}_\perp \frac{\theta_p^2 cK[k_{zq'}(\omega) + k_w]^2}{2\gamma\omega k_w} \mathbb{F}^{(h)}_{q,q'} \tag{9}$$

and the overlap of the e beam and the input fields is

$$\mathbb{F}^{(h)}_{q,q'} = \frac{\int f(\mathbf{r}_\perp)\tilde{\mathcal{E}}^{(h)}_{\perp q'}(\mathbf{r}_\perp)\tilde{\mathcal{E}}^*_{\perp q}(\mathbf{r}_\perp) d^2\mathbf{r}_\perp}{\int |\tilde{\mathcal{E}}_{\perp q}(\mathbf{r}_\perp)|^2 d^2\mathbf{r}_\perp}, \tag{10}$$

where $\mathbb{F}_{q,j} = \mathbb{F}^{(1)}_{q,j}$ with $m = 0$ in Eq. (6). Equation (8) describes the density bunching evolution of the e beam at the harmonics with arbitrary initial conditions on the bunching $a_q(0)$, velocity modulation $da_q(0)/dz$ and input field amplitudes $C_q(0)$. The second term on the left hand side of Eq. (8) is the contribution of the longitudinal space charge. Note that with the coupling turned off ($\mathbb{D}^{(h)}_{q,q'} = 0$), Eq. (8) describes the coupled harmonic oscillations of the density modes due only to longitudinal space-charge effects. This effect can become important, especially at lower energies, and may be useful for calculation of the density and velocity bunching amplitudes of the e beam over a drift before or after the undulator.

The coupling selection rules and resulting e beam modulations [Eq. (7)] that are excited in the interaction with a harmonic field input mode can be examined with a basis with the form

$$\tilde{\mathcal{E}}_{\perp q}(\mathbf{r}_\perp) = R^l_p(r) e^{il\phi}, \tag{11}$$

where the mode index takes on two values, $q = (p, l)$ corresponding to the radial (p) and azimuthal (l) modes. Assuming an axisymmetric e beam profile $f(\mathbf{r}_\perp) = f(r)$, the integral over ϕ in Eq. (10) is straightforward,

$$\mathbb{F}^{(h)}_{(p,l),(p',l')} \propto 2\pi\delta_{l',l\pm(h-1)}. \tag{12}$$

This shows how the coupling between azimuthal density modulation modes in the e beam, l, and the azimuthal modes in the EM field, l', depend on the harmonic number h and the direction of undulator polarization, $\pm$. In the simple case of an input EM mode with arbitrary l' introduced to the undulator at the fundamental frequency ($h = 1$), the corresponding azimuthal mode $l = l'$ is excited in the e beam. At the second harmonic frequency ($h = 2$), the axisymmetric EM field mode $l' = 0$ will generate a helically bunched e beam with azimuthal mode number $l = -1$ for an RH undulator and $l = 1$ for an LH undulator. Thus, an initially axisymmetric e beam and axisymmetric input EM field mode can be used to produce a helically microbunched e beam at the second harmonic (Fig. 1). It is interesting to note that the slowly varying amplitudes of the helical density distribution suggest an intriguing analogue with the manifestation of the Berry phase along the azimuthal coordinate [16,17].

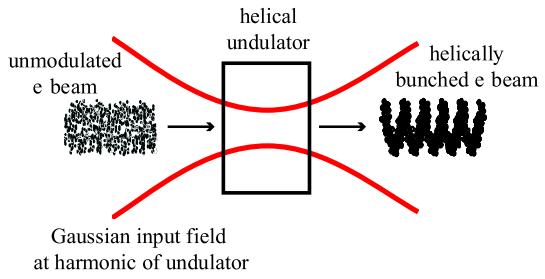

FIG. 1 (color online). Buncher device where the axisymmetric input field imprints a helical density and velocity modulation on the e beam through the harmonic interaction in a helical undulator.

The e beam density bunching is parametrized by the bunching factor [18]. To accommodate helical bunching of the e beam, we define a modified bunching factor $b_l(z)$ which incorporates the amplitude of bunching due to the lth discrete azimuthal mode:

$$b_l(z) = \frac{1}{n_0 \int f(\mathbf{r}_\perp) d^2\mathbf{r}_\perp} \int n_1(\mathbf{r}) e^{-il\phi} d^2\mathbf{r}_\perp. \tag{13}$$

This gives $b_l(z) = \delta_{l,0}$ when the density perturbation is $n_1(\mathbf{r}) = n_0 f(\mathbf{r}_\perp)$, i.e., complete longitudinal bunching at the $l = 0$ e beam mode. Helical e beam density bunching curves at the second harmonic are shown in Fig. 2 for three different values of the total input power of an $l' = 0$ Gaussian free-space mode at $2\pi c/\omega^{(2)} \simeq \lambda = 10.6$ μm. In each case, there is good agreement between the solutions to Eq. (8) with an LG basis [10] and 3D numerical particle tracking simulations performed with TREDI [19]

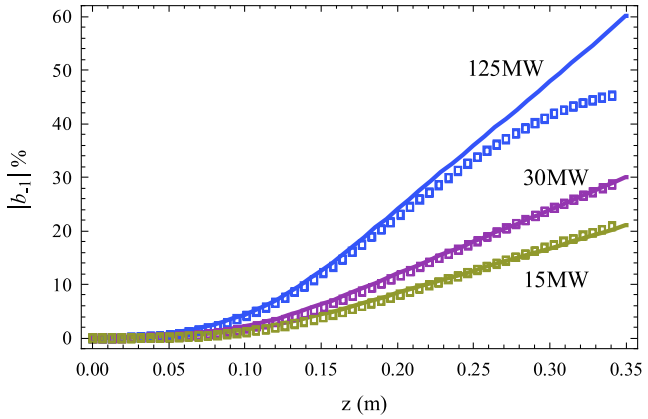

FIG. 2 (color online). Injection of a Gaussian input mode onto a Gaussian e beam for a RH undulator excites $l = -1$ density bunching at the second harmonic ($\lambda = 10.6$ μm). The associated helical bunching curves for a 350 μm spot size Gaussian mode with waist at $z = 0.15$ m on a $r_0 = 350$ μm e beam are in good agreement with TREDI simulations (points) with $\gamma = 26$, $K = 0.65$, $\lambda_w = 2$ cm.

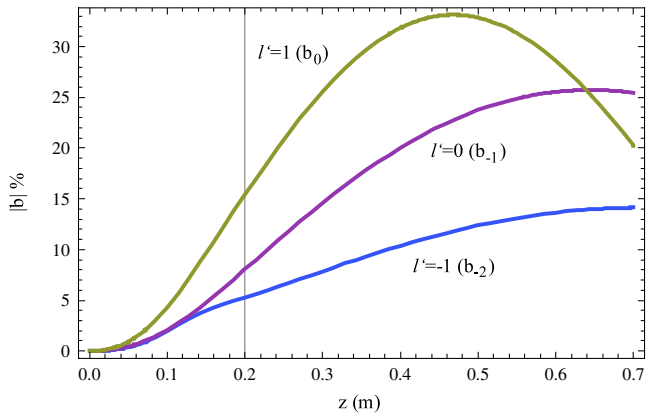

FIG. 3 (color online). Longitudinal space-charge effects included in bunching evolution for the injection of $l' = -1$, 0, and 1 modes onto a Gaussian e beam for a RH undulator at $h = 2$. The optical spot size is 500 μm for each mode, with the waist positioned halfway through the 20 cm undulator (vertical line). The beam displays the onset of plasma oscillations downstream. Input power is 15 MW and the e beam current is 300 A with $\gamma = 26$, $K = 0.65$, $\lambda_w = 2$ cm.

for dominant bunching at the $l = -1$ density mode. Significant bunching is observed near the exit of the 35 cm RH undulator with only 15 MW of input power. Bunching into modes $l \neq -1$ is negligible. Note that the analytic description assumes $r_0 \gg |\tilde{\mathbf{r}}_{\perp w}|$ but still works well in this case where $r_0 \sim 5|\tilde{\mathbf{r}}_{\perp w}|$. The departure of our linear theory from simulations (which include nonlinear aspects) is evident for very large bunching ($|b_l| > 35\%$), as in the case of 125 MW of input power.

The effects of space charge are ignored in Fig. 2, but can play a crucial role in the evolution of the microbunching. Figure 3 includes space-charge effects in the case of injection of $l' = -1$, $l' = 0$, and $l' = 1$ free-space LG modes with a Gaussian e beam in a RH undulator. The corresponding axial velocity modulation modes ($l = -2$, $l = -1$, and $l = 0$ modes excited in the e beam, respectively) manifest in the growth of the bunching factors downstream of the 20 cm undulator, which reach a maximum and then decrease due to space charge.

Maximum peak microbunching is achieved with the injection of the "natural" $l' = 1$ field, which bunches the beam into the $l = 0$ mode, i.e., longitudinally separated microbunches (b_0). This $l' = 1$ optical mode excites larger bunching than the other modes at the 2nd harmonic because it has larger resonant coupling to the e beam. This relates directly back to the 2nd harmonic FEL scenario where this optical mode achieves the highest gain [8]. In general for FELs with this coupling, a helical undulator with right (left) circular magnetic field polarization amplifies an $l' = h - 1$ ($l' = 1 - h$) azimuthal mode with left (right) circular polarization. The spin and orbital components of the photon angular momentum in the emitted photons in the FEL add since the projection of each onto the axis of propagation has the same sign. The $|l'| > 0$ EM modes described here are characterized by a null intensity on-axis, as expected [20–22]. Generation of intense light with OAM by helical beams in FELs is the subject of more detailed future work, and should include transverse betatron motion and emittance effects beyond the cold-beam model presented here.

This research was supported by grants from Department of Energy Basic Energy Science Contract No. DOE DE-FG02-07ER46272 and DE-FG03-92ER40693, and Office of Naval Research Contract No. ONR N00014-06-1-0925.

[1] P. Török and P. Munro, Opt. Express **12**, 3605 (2004).
[2] G. Gibson, J. Courtial, M. Padgett, M. Vasnetsov, V. Pas'ko, S. Barnett, and S. Franke-Arnold, Opt. Express **12**, 5448 (2004).
[3] E. Yao, S. Franke-Arnold, J. Courtial, M. J. Padgett, and S. M. Barnett, Opt. Express **14**, 13 089 (2006).
[4] M. F. Andersen, C. Ryu, P. Clade, V. Natarajan, A. Vaziri, K. Helmerson, and W. D. Phillips, Phys. Rev. Lett. **97**, 170406 (2006).
[5] A. Alexandrescu, D. Cojoc, and E. DiFabrizio, Phys. Rev. Lett. **96**, 243001 (2006).
[6] L. Allen, S. M. Barnett, and M. J. Padgett, *Optical Angular Momentum* (Institute of Physics, Bristol, 2003), ISBN 0750309016.
[7] L. Allen, M. W. Beijersbergen, R. J. C. Spreeuw, and J. P. Woerdman, Phys. Rev. A **45**, 8185 (1992).
[8] S. Sasaki and I. McNulty, Phys. Rev. Lett. **100**, 124801 (2008).
[9] E. Hemsing and J. B. Rosenzweig, J. Appl. Phys. (to be published).
[10] E. Hemsing, A. Gover, and J. Rosenzweig, Phys. Rev. A **77**, 063831 (2008).
[11] E. Hemsing, A. Marinelli, S. Reiche, and J. Rosenzweig, Phys. Rev. ST Accel. Beams **11**, 070704 (2008).
[12] N. Vinokurov, *Proceedings of the 10th International Conference on Particle Accelerators, Institute Siziki Zysokikh Energie, Serpukhov, U.S.S.R.*, Vol. 2, p. 454 (1977).
[13] Y. Pinhasi and A. Gover, Phys. Rev. E **51**, 2472 (1995).
[14] E. Hemsing, A. Gover, and J. Rosenzweig, Phys. Rev. A **77**, 063830 (2008).
[15] J. D. Jackson, *Classical Electrodynamics* (J. Wiley and Sons, New York, 1999), 3rd ed.
[16] M. V. Berry, Proc. R. Soc. A **392**, 45 (1984).
[17] M. J. Padgett and J. Courtial, Opt. Lett. **24**, 430 (1999).
[18] J. Wu, Z. Huang, and P. Emma, Phys. Rev. ST Accel. Beams **11**, 040701 (2008).
[19] L. Giannessi, P. Musumeci, and M. Quattromini, Nucl. Instrum. Methods Phys. Res., Sect. A **436**, 443 (1999).
[20] W. Colson, IEEE J. Quantum Electron. **17**, 1417 (1981).
[21] G. Geloni, E. Saldin, E. Schneidmiller, and M. Yurkov, Nucl. Instrum. Methods Phys. Res., Sect. A **581**, 856 (2007).
[22] E. Allaria, F. Curbis, M. Coreno, M. Danailov, B. Diviacco, C. Spezzani, M. Trovó, and G. DeNinno, Phys. Rev. Lett. **100**, 174801 (2008).